Detection of drug-induced cellular changes using confocal Raman spectroscopy on patterned single-cell biosensors

Ryan Buckmaster,[a] Fareid Asphahani,[a] Myo Thein,[b] Jian Xu[b] and Miqin Zhang*[a]

Received 13th January 2009, Accepted 21st April 2009
First published as an Advance Article on the web 30th April 2009
DOI: 10.1039/b900420c

We report on a cell-based biosensor application that utilizes patterned single-cell arrays combined with confocal Raman spectroscopy to observe the time-dependent drug response of individual cells in real time. The patterned single-cell platform enables individual cells to be easily located and continuously addressable for Raman spectroscopy characterization of biochemical compositional changes in a non-destructive, quantitative manner so that discrete cellular behavior and cell-to-cell variations are preserved. In this study, human medulloblastoma (DAOY) cells were exposed to the common chemotherapeutic agent etoposide, and Raman spectra from patterned cells were recorded over 48 hours. It was found that 87.5% of the cells monitored exhibited a sharp decrease in DNA and protein associated peaks 48 hours after drug exposure, corresponding to cell death. The remaining 12.5% of the cells showed little to no reduction in key Raman biomarkers, indicating their drug resistance. Furthermore, the patterned cell population showed a very similar response to etoposide as confluent cell cultures, as confirmed by flow cytometry. Finally, patterned cells were assessed with TUNEL assay for apoptosis due to DNA fragmentation after etoposide exposure. The results agree well with those from the Raman spectroscopy analysis. This combined biosensor–Raman platform provides a quick, simple way to assess cell responses to chemical and biological agents with high throughput and can be potentially used for a wide variety of biomedical applications such as pharmaceutical drug discovery, toxin tests, and biothreat detection.

Introduction

Cell-based biosensors utilize living cells as sensing elements capable of detecting and responding to biological and chemical agents as diverse as bacteria, viruses, toxins, and pharmaceutics, offering tremendous advantages for many biomedical and environmental applications.[1,2] Many current cell-based sensors measure the averaged behavior of groups of cells that often masks crucial cell-to-cell differences.[3,4] The behavior and response of "outlier" cells far from the average cell population response, potentially lost in averaged bulk measurements, can be of critical importance in the study of cellular biology and disease such as drug resistance in cancers and gene expression variations within clonal populations.[3,5,6] By developing single-cell based biosensors to study individual cell behavior, the limitations inherent in multiple-cell based platforms can be overcome, allowing a better understanding of the entire cellular population.[7]

Recently, microarrays of single-cell based sensors are rapidly emerging as a promising technology for studying cellular behavior because they are uniquely capable of recording cell-to-cell differences while retaining advantageous features of conventional cell-based biosensors such as noninvasive and instantaneous detection, high throughput, acute sensing efficiency, and reduced sample sizes.[8,9] They are addressable through a multitude of optical and electronic characterization techniques that usually monitor whole cell responses to a limited range of changes such as pH alterations due to metabolic changes, gene and protein expression related to cell signaling, or cell membrane properties due to adhesion, spreading, and motility.[10–12] It is desirable to establish a non-destructive measurement technique capable of monitoring a myriad of cellular mechanisms and reactions to stimuli over long periods of time without damaging the cells during measurements. Confocal Raman spectroscopy, a quantitative and non-destructive optical technique based on inelastic scattering of laser photons by molecular vibrations of biopolymers that is capable of detecting information on the biochemical composition of cells (*e.g.* amino acids and proteins, lipids, and nucleic acids),[13,14] offers this advantage and has been previously used to study cellular events such as chemical changes and cell death induced by drugs[15] or toxins,[16,17] as well as cellular changes at different time points in the cell cycle.[18] Raman spectroscopy does not require chemical tags to gain insight into the physiological processes occurring within a cell, leaving cellular functions unaltered during observations and available for repeated monitoring of time-dependent events of the same cell.[19] For these reasons, Raman spectroscopy is suitable and often ideal in many biological applications that require comprehensive information that characterizes the cellular biochemical state.

Cancer–drug interactions are particularly interesting due to the multitude of possible outcomes in cellular response including apoptosis, quiescence, and acquired drug immunity. For

[a]*Department of Materials Science & Engineering, University of Washington, 302L Roberts Hall, Seattle, WA, 98195-2120, USA. E-mail: mzhang@u.washington.edu; Fax: (+1 206) 543-3100; Tel: (+1 206) 616-9356*
[b]*Department of Engineering Science and Mechanics, Pennsylvania State University, University Park, Pennsylvania, 16802, USA*

instance, acquired chemotherapeutic drug resistance is believed to be linked to the degree of intrinsic sensitivity of DNA damage-induced apoptosis.[20] Thus, a technique such as confocal Raman that provides extensive quantitative and time-dependent information about biological processes from each single cell among a larger population would be very useful to better understand these phenomena, which could lead to the development of better cancer treatment options. In this study, we combined the capability of confocal Raman spectroscopy with our previously established single-cell patterning technique[21] for the detection of time-dependent effects of etoposide, an anticancer drug, on a population of isolated DAOY human medulloblastoma single cells. Etoposide is a standard chemotherapeutic topoisomerase II-α inhibitor,[22] and DAOY cells are representative of medulloblastoma which accounts for over 20% of pediatric brain tumors.[23] To demonstrate the present technique, Raman analysis from our single-cell based biosensor platform was used for the detection of cellular apoptosis, a typical analysis for anticancer drug screening, and was compared to the current standard viability detection techniques of flow cytometry and TdT-dUTP terminal nick end labeling (TUNEL) assays.

Experimental

Materials

The chemicals used for substrate modification include 11-mercaptoundecanoic acid 95% (11-MUA), *N*-hydroxysuccinimide 97% (NHS), 1-ethyl-3-(3-dimethylamino-propyl) carbodimide (EDAC) (Sigma, St. Louis, MO, USA), 2-[methoxy-(polyethyleneoxy)propyl] trimethoxysilane (PEG) (Mw = 460–590 Dalton; Gelest, Morrisville, PA, USA), Nano™ Remover PG (MicroChem, Newton, MA, USA), and NanoStrip™ 2X (Cyantek, Fremont, CA, USA). Cell culture materials include paraformaldehyde and glutaraldehyde (Sigma St. Louis, MO, USA), lysine-arginine-glycine-aspartic acid (KRGD) peptide (SynBioSci, Livermore, CA, USA), Opti-MEM® I Reduced-Serum medium (w/o phenol red), 1X phosphate buffered saline solution (PBS), heat-inactivated fetal bovine serum (FBS), penicillin–streptomycin–neomycin (PSN) antibiotic 100X mixture, trypsin–EDTA (ethylenediamine tetra-acetic acid) (Invitrogen, Carlsbad, CA, USA), and DAOY human medulloblastoma cell line (ATCC, Manassas, VA, USA). Materials for the flow cytometry assay include phenol-free Dulbecco's Modified Eagle Medium (DMEM), 1X PBS, and propidium iodide stain (Invitrogen, Carlsbad, CA, USA). For the TUNEL staining, the APOBrdU TUNEL Assay Kit with Alexa Fluor 488 antiBrdU and Prolong® Gold antifade reagent with DAPI (Invitrogen, Carlsbad, CA, USA) was used.

Surface modification and cell culture

Gold-patterned silicon oxide substrates were fabricated with arrays of 40 μm spaced 20 μm × 20 μm squares and chemically modified using methods previously established with minor modifications.[21,24,25] Briefly, the substrates were placed in NanoStrip™ 2X at room temperature for 40 min to produce a hydroxyl layer on the SiO_2 regions, cleaned and placed into a 20 mM solution of 11-MUA for 16 h to form a self-assembled monolayer (SAM) on the gold squares. The substrates were then immersed in a solution containing 3 mM PEG and 1% triethylamine in anhydrous toluene at 60 °C for 18 h. The substrates were then immersed in an aqueous solution of 30 mM NHS and 150 mM EDAC for 30 min at room temperature to attach the NHS ester to the –COOH terminus of the SAM for later conjugation to the KRGD peptides to enhance cell adhesion. The substrates were transferred to a 24-well plate, sterilized with ethanol for 15 min, rinsed with DI water, and exposed to KRGD peptides in an 8.2 pH PBS solution at a concentration of 0.05 mg mL^{-1} at room temperature for 1 h to conjugate the KRGD lysine groups to the NHS groups on the gold bound SAM. To remove loosely bound moieties from the surface after each step of surface modification, the substrates were rinsed with the original solvent and DI water, respectively.

DAOY cells were cultured in Opti-MEM® media supplemented with 1% FBS and 1% PSN in 75 cm^2 flasks at 37 °C in a humidified atmosphere with 5% CO_2. For cell seeding on the modified substrates, cells were detached from the culture flasks at near confluency by washing the cells twice with 7.4 pH PBS and incubating in 2 mL of trypsin–EDTA solution for 5 min. Fresh medium was then added to dilute the cells to a concentration of 2×10^5 cells mL^{-1}. Upon the completion of the surface modification described above, 0.5 mL of the cell solution was applied to each surface and incubated at 37 °C for 12 h.

Raman spectroscopy

Twelve hours after seeding the surfaces with DAOY cells, the substrates were placed in a Petri dish containing 10 mL of the same cell culture medium over a stage heater set at 37 °C and covered with mineral oil to prevent evaporation and seal the cell culture medium from outside contaminates. A Renishaw inVia Raman spectrometer attached to a Leica DMLM upright microscope equipped with a 63× water immersion objective and 785 nm laser at 30 mW power with a laser spot size 16 μm long, 4 μm wide, and 25 μm deep in the axial direction was used to collect all spectra. The laser spot was centered on the cell and the spectra were taken for 120 s from eight single cells on 20 μm × 20 μm squares in three identical experiments. After the initial set of spectra was collected, 20 μL of 5 mM etoposide dissolved in cell culture media was added resulting in a 10 μM etoposide concentration in the cell chamber medium. Spectra were retaken from the same cells every 12 hours. Spectra from a modified gold square unoccupied by cells were then subtracted from the acquired cell spectra to remove the spectral contributions of the substrate and cell medium. The baseline was then subtracted using a multi-point cubic spline. As all of the cells had a uniformly spread area, normalization was not performed. Peak fitting was performed using the peak fitting option of the Renishaw WiRE 2.0 program assuming Gaussian line shapes.

Flow cytometry

The viability of etoposide-treated cells was determined by using propidium iodide to stain non-viable cells characterized by standard flow cytometry. 8×10^5 DAOY cells were plated in each well of a standard 12-well plate and allowed 12 h to seed resulting in a confluent culture. After 12 hours, the culture medium was replaced with fresh medium containing 10 μM of

etoposide. A separate set of control cultures without etoposide was kept under the same conditions. For every 12 h up to 48 h, one well was harvested and the cells were subsequently stained with propidium iodide per the manufacturer's protocol. The stained cells were then put on ice and immediately analyzed by flow cytometry. Data was then processed using the Flow Jo software package.

TUNEL staining assay

Apoptosis of DAOY cells was determined by the TUNEL staining assay, which is used to identify DNA fragmentation by fluorescently labeling DNA strand breaks. Cell arrays were fixed by washing with ice cold 7.4 pH PBS buffer solution and fixed for 15 min with ice cold 1% paraformaldehyde in PBS solution of 7.4 pH, followed by 20 min in ice cold absolute ethanol, and finally rinsed in 7.4 pH PBS buffer solution. Cell staining was carried out per the manufacturer's protocol. After fixation, the cells were mounted on #1 thickness cover slips using one drop of Prolong® Gold DAPI stain mounting reagent and allowed to cure in the dark for 24 h. Surfaces were then imaged using a 40× dry lens on a Delta Vision microscope (Issaquah, WA, USA) using an appropriate filter set with all images taken under the same conditions. TUNEL intensity of a given cell was then quantified using Image J software.

Results and discussion

Cell adhesion on gold microarrays

To record individual cell resolved spectral measurements in real time, individual cells were first patterned through natural cell adhesion to predefined locations by a method similar to one reported previously.[21] Briefly, DAOY cells were immobilized on 40 μm spaced 20 μm × 20 μm gold squares over SiO_2 substrates by chemically modifying the surface with a SAM of 11-MUA conjugated to KRGD peptides to selectively enhance single-cell adhesion to gold regions while repelling cells from the SiO_2 background with a PEG SAM. The spacing and sizes of the squares were chosen to maximize the number of single cells and avoid the formation of bridging cell clusters. Fig. 1a shows an illustration of the surface modification chemistry prior to cell seeding, and Fig. 1b shows a high magnification region of a typical array of patterned DAOY cells. DAOY cells patterned on the modified Au/SiO_2 substrates were seen to exhibit excellent single-cell patterning and spreading to conform to the shape of the gold squares. The well spread morphology and conformation of the patterned DAOY cells to the shape of the functionalized gold squares is a result of the affinity between the $\alpha_v\beta_3$ integrin expressed on DAOY cells[26] and the RGD peptide sequence[27] that are covalently-bound to the gold surface. The PEG modified SiO_2 background area effectively prevented the DAOY cells from spreading outside of the peptide-functionalized gold squares. Previous results have shown that cells patterned in this manner can retain viability for several days.[28] Raman spectral analysis of those patterned single cells (not shown) and TUNEL staining results (Fig. 5, to be discussed later) have also verified that cells patterned on such surfaces remained viable for several days, which is essential for cells to serve as sensing elements.

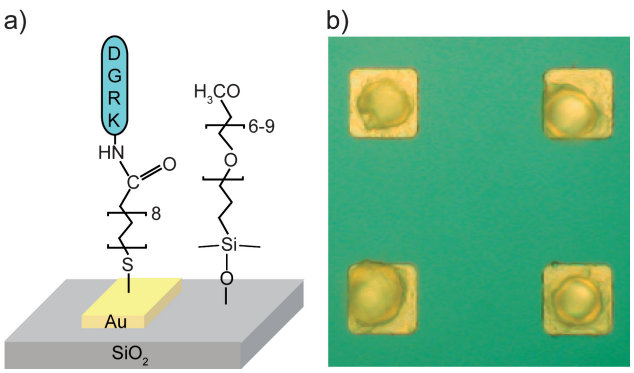

Fig. 1 (a) Schematic of the final surface modification of gold-patterned silicon oxide substrate for subsequent single-cell adhesion. (b) Optical differential interference contrast (DIC) image of patterned DAOY cells on the surface-modified 20 μm × 20 μm gold squares with 40 μm spacing between squares.

Single-cell confocal Raman spectroscopy

To observe cellular level reactions from patterned DAOY cells after exposure to etoposide, confocal Raman spectroscopy was used to measure biomolecular vibrations representative of changes in the biochemical makeup of individual patterned cells. Eight well spread single cells patterned on the array substrate placed in a Petri dish of cell culture medium were located using the integrated microscope of the Raman instrument, and Raman spectra were taken with the laser centered on each cell prior to (0 h) and every 12 h up to 48 h after inoculating the medium with a 10 μM concentration of etoposide. A dose of 10 μM is anticipated to induce apoptosis in a majority of DAOY cells within two days.[29] Data analysis was performed after removing the spectral contribution of the cell culture medium and substrate by subtracting the background. Since the spread morphology of the patterned cells was constant throughout the duration of the experiment and each individual cell's responses were referenced to its 0 h measurement, no subsequent normalization was necessary. Measurements of an unoccupied modified gold square recorded every 12 h showed no noticeable changes in spectra or intensity.

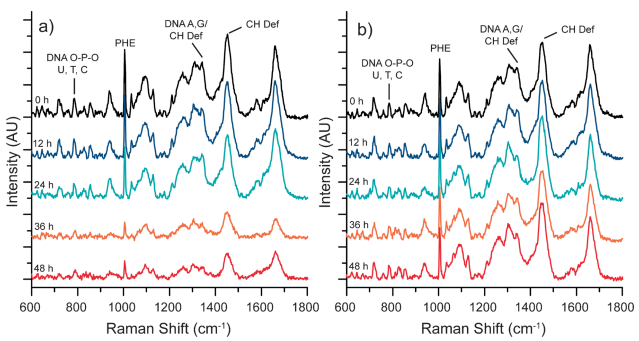

Fig. 2 Raman spectra for two representative cells acquired prior to (0 h) and every 12 hours after etoposide exposure. (a) Raman spectra of cell 1, suggesting that the cell died after 36 hours. (b) Raman spectra of cell 5, indicating that the cell was viable over the course of the experiment.

Fig. 2 shows two sets of time resolved spectra over 48 hours for two of the eight individual cells (cell 1 and cell 5), which are representative of two general but variant responses observed among the cells exposed to etoposide. For cell 1 (Fig. 2a), the Raman spectrum remained unchanged for the first 24 hours after etoposide exposure, after which there was a substantial decrease in the 782/788 cm^{-1} peak associated with nucleic acids and the DNA backbone, respectively, which suggests the beginning of DNA fragmentation during apoptosis. After 36 hours, the overall Raman peak intensities decreased by 30–50%. For cell 5 (Fig. 2b), on the other hand, while several small changes were observed post etoposide exposure, the cell retained the overall spectral profile over 48 h, similar to the spectrum before etoposide exposure. While the resilience of cell 5 to etoposide differs from most of the other 23 cells examined in this study, such differences among individual cells within even nominally clonal cell populations are of critical importance in biological systems.[3,4] For our current sample sizes of 24 cells, subpopulations down to 10% of the total can be detected over 90% of the time. By using larger arrays and automated data collection, even smaller subpopulations of interest can be reliably identified and monitored.

It should be noted that all cells examined before etoposide exposure (0 h) had Raman spectra typical of healthy cells, consistent with previously reported cellular Raman spectra for other mammalian cell types.[16,18,30] The Raman spectra of cells that underwent apoptosis and subsequent cell death after etoposide exposure showed apparent changes, most notably a significant decrease in the overall spectral intensity (as seen in Fig. 2a). Observations made under a microscope during the course of the Raman analysis showed that, accompanying the Raman spectral intensity reduction, the cells exhibited rougher morphology and blebs.

To better understand the molecular changes occurring in the patterned DAOY cells, the collected Raman spectra of one of the three identical sets of eight patterned single cells were examined in more detail. Previous studies have compiled peak assignments of major cellular components[30] that have been used for peak fitting of the collected Raman spectra. Fig. 3 shows the changes in the peak intensities of five key biochemical components for eight individual DAOY cells over 48 hours, as well as for a population average of all eight patterned cells. The plotted cellular components in Fig. 3 include uracil (U), thymine (T), and cytosine (C) ring vibrations at 782 cm^{-1} corresponding to the nucleic acid components of DNA and RNA, the O–P–O phosphodiester DNA backbone at 788 cm^{-1}, ring vibrations of phenylalanine (Phe) at 1005 cm^{-1} corresponding to proteins, DNA nucleic acids adenine (A) and guanine (G) and C–H deformation in proteins at 1342 cm^{-1}, and C–H deformation in all cellular components at 1450 cm^{-1}. For easy comparison, the peak intensities acquired at time points of 12, 24, 36 and 48 h were normalized to the initial intensities taken immediately before etoposide exposure (0 h). For the two cases where cells had detached before the 48 h measurement (cells 6 and 8), the peak intensity values were set to zero for the averaged cell peak values at 48 h.

Several trends in changes of peak intensities after the etoposide exposure are evident in Fig. 3. Most cells underwent apoptosis and died after 36 hours, as indicated by the significant reduction in Raman peak intensity for all or most of the five components. These spectral changes after etoposide exposure are consistent with those observed at late stage apoptosis.[31,32] Particularly, the Phe peak at 1005 cm^{-1} and the protein C–H deformation and A, G nucleic acid peak at 1342 cm^{-1} exhibited sharp intensity decreases for all but one cell at 36 h and 48 h time points, making these excellent biomarkers of cell death. However, exceptions to the expected normal response were also observed, as exemplified by one cell (cell 5) that appeared to have overcome the effects of etoposide at the current dose. Given the intrinsic resistance of related glioma type cells to apoptosis, the survival of some medulloblastoma cells to etoposide exposure is expected.[33,34] Studying the behavior of these resistant cells is critically important in highly effective pharmaceutical drug development and screening.

The current technique has also demonstrated great sensitivity to subtle, but interesting cellular response changes that would otherwise be missed using standard assays. While all the selected average peak values followed the same trend of decreasing by over 50% upon apoptosis and cell death (Fig. 3), the 788 cm^{-1} O–P–O DNA backbone stretch and 782 cm^{-1} U, T, C peaks showed the greatest variation among each of the eight cells in the population to eventually arrive at this overall response over the 48 h duration. Some variation can be expected as the concentration of cellular DNA varies spatially within the nucleus and temporally due to ongoing cellular processes such as mitosis, gene expression, and apoptosis, indicative of changes in cellular function and state. Thus, any changes in nuclear shape and size will affect the corresponding Raman peak intensities. However, variations in nucleic acid peak intensities due to actual changes in the biochemical state of the patterned cells, such as increases in DNA levels consistent with DNA replication as cells prepare for mitosis[18,30] or DNA level decreases due to an event such as apoptosis,[16] are much greater in magnitude.

Additionally, it was optically observed that most cells remained fully spread on the functionalized gold squares after 48 hours despite the significant loss of cellular mass, as indicated by the decrease in the 1450 cm^{-1} peak intensity. However, two cells detached from the surface (cells 6 and 8) after showing rapid reduction in Raman peak intensities at the 36 h measurement. Whether the cellular detachment was a random event or indicative of differing biological changes between the dying cells is unknown at present. These findings illustrate the advantage of the continued real-time analysis provided by this technique, where time-dependent cellular responses such as DNA replication and cell detachment can be easily observed.

Based on the Raman spectral analysis, cell death occurs not as a slow degradation of biomolecules but a relatively fast singular event. This stands in some contrast to the reports of A549 carcinoma epithelia cells exposed to Triton X-100 that underwent a slow death process drawn out over 48 hours.[16] However, it should be noted that these results were obtained from the averaged response of non-patterned cells that might be at different cellular states moving towards apoptosis. Additionally, different cell lines may also exhibit different cellular responses. In another report, the Raman analysis of an individual A549 cell exposed to Triton X-100 showed spectral changes associated with cell death over 7 hours,[35] more similar to what we have observed in this study. Still, the time lag of 12–24 hours before the observation of

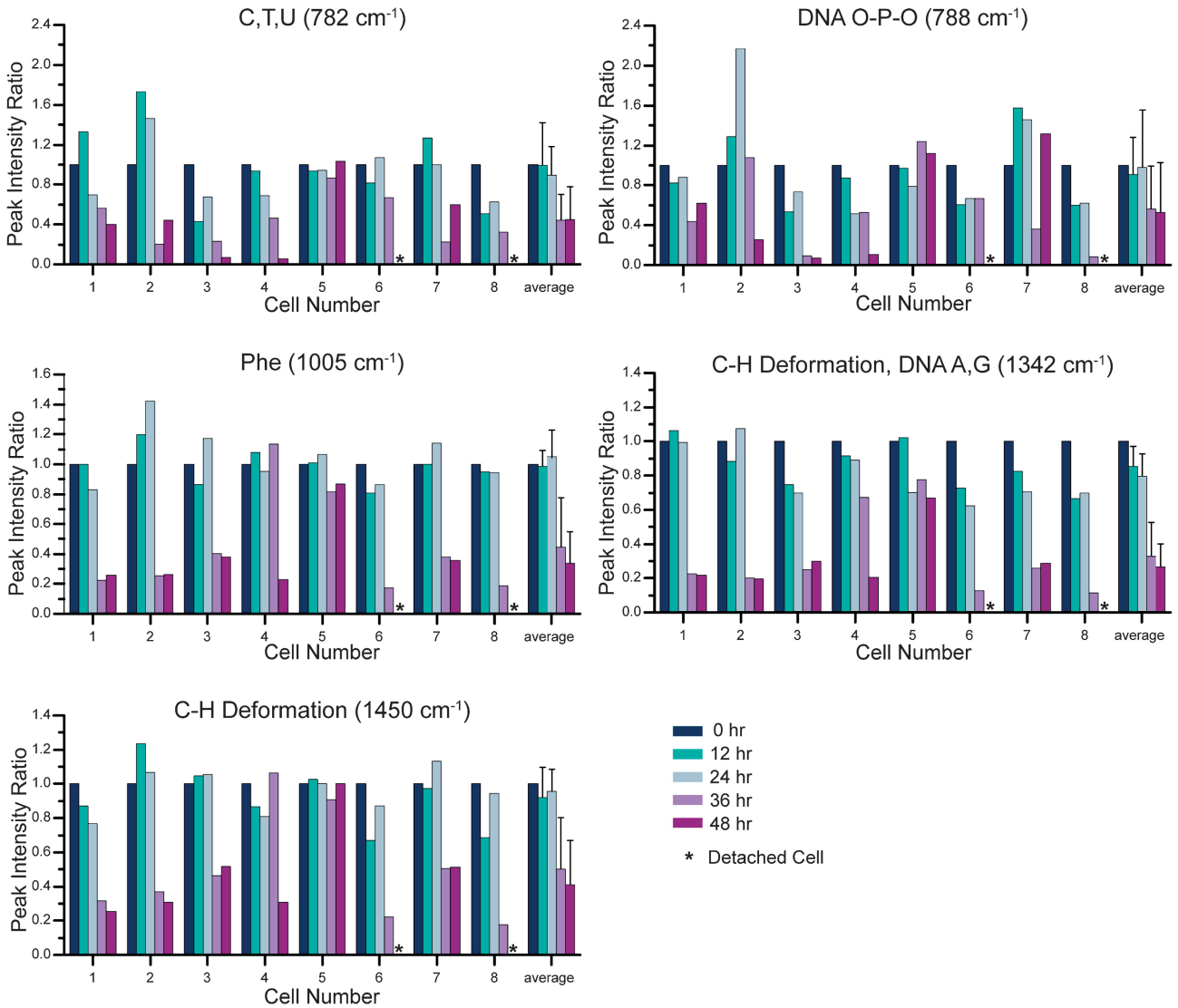

Fig. 3 Changes in intensity of selected Raman peaks of sampled patterned cells before and every 12 hours for 48 hours after etoposide exposure. Peaks are displayed as a ratio to the initial intensities (0 h) for each individual cell.

significant effects of the etoposide is not unexpected given the mechanism of action of the drug. Etoposide binds to the DNA chain and causes DNA strand breaks during DNA replication resulting in apoptosis.[36] Thus, only when the DAOY cells begin to undergo DNA replication will the etoposide cause DNA strand to breaks, triggering apoptosis.

Comparative cell viability assay using flow cytometry

To validate this single-cell platform as a means to examine cellular behavior in response to analytes, a comparison was made between the Raman spectral analysis results of a larger population of 24 cells and a standard flow cytometry-based viability assay. For flow cytometry analysis, confluent cultured cells were harvested at 0, 12, 24, 36 and 48 h after etoposide exposure and stained with propidium iodide (PI), a marker of cell viability. Since PI is not able to penetrate the membrane of healthy cells, non-viable and dead cells can be identified by the bright PI marker fluorescence.[37] For the patterned cells, the 1342 cm^{-1} A, G and protein C–H deformation peak was chosen as a comparative marker due to nucleic acid and protein contributions making it a good indicator of apoptosis and cell death, as previously shown in Fig. 3. Raman spectra were collected at 0, 12, 24, 36 and 48 h after etoposide exposure as detailed in previous sections. Fig. 4 compares the results of the flow cytometry and the 1342 cm^{-1} Raman peak by showing the PI fluorescence flow cytometry histograms of standard cultured cells (Fig. 4a) and the Raman 1342 cm^{-1} peak intensity histograms of patterned single cells (Fig. 4b). In both sets of histograms, the dotted lines denotes the criteria used for determining whether a cell was viable or not. This determination was used in Fig. 4c, which shows the normalized viability of the cultured and patterned cells based on the PI and Raman measurement in Fig. 4a and Fig. 4b, respectively.

The histograms in Fig. 4a and 4b demonstrate good qualitative agreement with increasing number of cells showing responses indicative of apoptosis caused by etoposide exposure as time increases. The flow cytometry results show a continual reduction

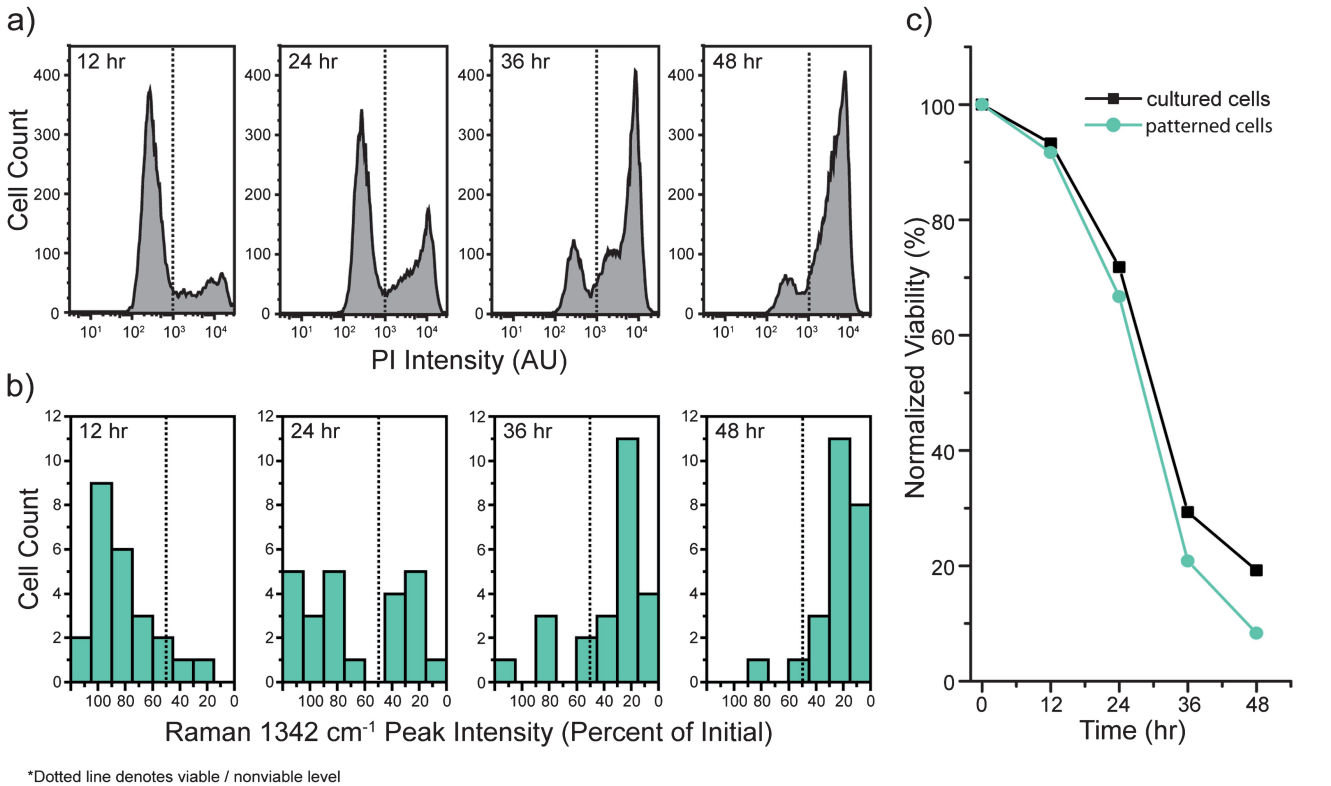

Fig. 4 (a) Flow cytometry PI fluorescence intensity histograms of DAOY cultured cells at 12, 24, 36, and 48 h after etoposide exposure. (b) 1342 cm^{-1} Raman peak (DNA A, G, protein C–H deformation) intensity histograms of $n = 24$ single patterned cells exposed to etoposide. (c) Normalized viability of cultured DAOY cells determined by PI intensity (squares) and patterned DAOY cells determined by the Raman 1342 cm^{-1} peak intensity (circles).

in viable cells as higher PI fluorescence intensity was detected over the 48 hour time course, with a particularly dramatic increase in cell nonviability between 24 and 36 h. For the patterned cells, the 1342 cm^{-1} Raman peak exhibited a sharp decrease in intensity, indicating cell death, between 24 and 36 h. The behavior of the two populations also demonstrated excellent quantitative agreement, as indicated by the viability curves in Fig. 4c. Overall, the trends of the 1342 cm^{-1} Raman peak of the patterned cells and the viability of confluent cell cultures correlated well, suggesting that changes in Raman intensity can be used to predict the overall viability of larger number of cells and that the patterned DAOY cells behave similarly to confluent cell cultures.

Assessment of apoptosis using TUNEL assay

Finally, the patterned DAOY cells were stained with TUNEL to further confirm the results of the Raman experiments. In TUNEL staining, the ends and nicks of DNA strands are fluorescently labeled to identify apoptotic cells by their greater fluorescence signals due to DNA fragmentation.[38] Fig. 5a shows typical DAOY cells fluorescently stained with DAPI and TUNEL from the control (top panel, no etoposide exposure) and etoposide exposed (bottom panel) groups. DAPI counter staining was carried out to identify the cell nucleus. For the TUNEL staining, the control cell showed low TUNEL intensity, while the cells exposed to etoposide exhibited significantly greater TUNEL fluorescence due to a large number of DNA strand breaks, suggesting apoptosis. Fig. 5b shows a histogram of the number of cells from the control and etoposide groups *versus* the integrated TUNEL intensity for $n = 24$ cells. Corresponding to the optical image in Fig. 5a, cells inoculated with the drug exhibited a higher TUNEL intensity indicative of reduced viability due to DNA strand breaks caused by the etoposide exposure. These results agreed well with the Raman spectral analysis that also showed DNA fragmentation and reduced cell viability from etoposide exposure.

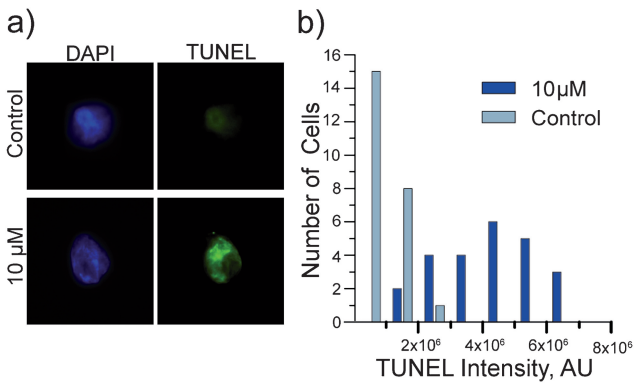

Fig. 5 Results of TUNEL staining of patterned DAOY cells. (a) DAPI (blue) and TUNEL (green) fluorescence images of typical control and etoposide exposed cells. (b) Histogram of TUNEL intensities for control and etoposide exposed cells for $n = 24$ cells examined.

Conclusions

Single-cell patterned microarrays of DAOY medulloblastoma cells combined with confocal Raman spectroscopy characterization technique were found to be capable of monitoring the apoptotic response of individual cells to etoposide over time. Raman peaks representing various cellular components in the DAOY cells diminished over 48 h after etoposide exposure. Although most of the cells died within 36 hours, a small number of cells were found to be capable of resisting or recovering from the drug effect. Such cell-to-cell differences in a population of identical cells can be best revealed by the current technique due to its ability to examine cells individually in real time. Additionally, the results of this technique were also found to be consistent with the results provided by conventional techniques such as flow cytometry and TUNEL staining assays, suggesting that the patterned cells behave similarly to confluent cells in culture. With the use of larger single-cell arrays, this technique can be used to detect and analyze even smaller subpopulations, further enhancing the value of this technique to track individual cell-to-cell differences.

Acknowledgements

This work is supported by National Institutes of Health (NIH/GMS R01GM075095). The authors thank the University of Washington NanoTech User Facility for access to the Renishaw inVia Raman microscope, Dr Paul Wallace of the NanoTech User Facility for his technical assistance, University of Washington Keck Center for use of the DeltaVision microscope, and Ms Kandy Yeung and Mr Johnson Tey for lab assistance.

References

1 J. J. Pancrazio, J. P. Whelan, D. A. Borkholder, W. Ma and D. A. Stenger, *Ann. Biomed. Eng.*, 1999, **27**, 697–711.
2 L. Lorenzelli, B. Margesin, S. Martinoia, M. T. Tedesco and M. Valle, *Biosens. Bioelectron.*, 2003, **18**, 621–626.
3 J. M. Levsky and R. H. Singer, *Trends Cell Biol.*, 2003, **13**, 4–6.
4 C. S. Chen, X. Y. Jiang and G. M. Whitesides, *MRS Bulletin*, 2005, **30**, 194–201.
5 R. Bahar, C. H. Hartmann, K. A. Rodriguez, A. D. Denny, R. A. Busuttil, M. E. T. Dolle, R. B. Calder, G. B. Chisholm, B. H. Pollock, C. A. Klein and J. Vijg, *Nature*, 2006, **441**, 1011–1014.
6 G. V. Tolstonog, I. V. Belichenko-Weitzmann, J. P. Lu, R. Hartig, R. L. Shoeman, U. Traub and P. Traub, *DNA Cell Biol.*, 2005, **24**, 680–709.
7 M. Veiseh, O. Veiseh, M. C. Martin, C. B. Ertozzi and M. Q. Zhang, *Biosens. Bioelectron.*, 2007, **23**, 253–260.
8 P. McFadden, *Science*, 2002, **297**, 2075–2076.
9 M. Veiseh, B. T. Wickes, D. G. Castner and M. Q. Zhang, *Biomaterials*, 2004, **25**, 3315–3324.
10 F. Asphahani and M. Zhang, *Analyst*, 2007, **132**, 835–841.
11 M. E. Bosch, A. J. R. Sanchez, F. S. Rojas and C. B. Ojeda, *Comb. Chem. High Throughput Screening*, 2007, **10**, 413–432.
12 C. Q. Yi, Q. Zhang, C. W. Li, J. Yang, J. L. Zhao and M. S. Yang, *Anal. Bioanal. Chem.*, 2006, **384**, 1259–1268.
13 D. Naumann, *App. Spectrosc. Rev.*, 2001, **36**, 239–298.
14 I. Notingher, *Sensors*, 2007, **7**, 1343–1358.
15 C. A. Owen, J. Selvakumaran, I. Notingher, G. Jell, L. L. Hench and M. M. Stevens, *J. Cell. Biochem.*, 2006, **99**, 178–186.
16 S. Verrier, I. Notingher, J. M. Polak and L. L. Hench, *Biopolymers*, 2004, **74**, 157–162.
17 I. Notingher, C. Green, C. Dyer, E. Perkins, N. Hopkins, C. Lindsay and L. L. Hench, *J. R. Soc. Interface*, 2004, **1**, 79–90.
18 K. W. Short, S. Carpenter, J. P. Freyer and J. R. Mourant, *Biophys. J.*, 2005, **88**, 4274–4288.
19 I. Notingher, S. Verrier, H. Romanska, A. E. Bishop, J. M. Polak and L. L. Hench, *Spectrosc.–Int. J.*, 2002, **16**, 43–51.
20 P. Savage, J. Stebbing, M. Bower and T. Crook, *Nat. Clin. Pract. Oncol.*, 2009, **6**, 43–52.
21 M. Veiseh, O. Veiseh, M. C. Martin, F. Asphahani and M. Q. Zhang, *Langmuir*, 2007, **23**, 4472–4479.
22 A. M. Karch and J.B. Lippincott Company., Lippincott, Philadelphia, PA, Editon edn., 1995, p. v.
23 D. Ellison, S. Clifford, A. Gajjar and R. Gilbertson, *Eur. J. Paediatr. Neurol.*, 2003, **7**, 53–66.
24 M. Veiseh, M. H. Zareie and M. Q. Zhang, *Langmuir*, 2002, **18**, 6671–6678.
25 M. Veiseh, B. T. Wickes, D. G. Castner and M. Zhang, *Biomaterials*, 2004, **25**, 3315–3324.
26 R. Stolarek, C. Gomez-Manzano, H. Jiang, G. Suttle, M. G. Lemoine and J. Fueyo, *Cancer Gene Therapy*, 2004, **11**, 713–720.
27 E. Ruoslahti, *Annu. Rev. Cell. Dev. Biol.*, 1996, **12**, 697–715.
28 M. Veiseh and M. Zhang, *J. Am. Chem. Soc.*, 2006, **128**, 1197–1203.
29 A. J. Janss, A. Cnaan, H. Q. Zhao, A. Shpilsky, C. Levow, L. Sutton and P. C. Phillips, *Anti-Cancer Drugs*, 1998, **9**, 641–652.
30 I. Notingher, S. Verrier, S. Haque, J. M. Polak and L. L. Hench, *Biopolymers*, 2003, **72**, 230–240.
31 K. Vermeulen, D. R. Van Bockstaele and Z. N. Berneman, *Ann. Hematol.*, 2005, **84**, 627–639.
32 P. Clarke, *Anat. Embryol. (Berl)*, 1990, **181**, 195–213.
33 D. S. Ziegler, A. L. Kung and M. W. Kieran, *J. Clin. Oncol.*, 2008, **26**, 493–500.
34 D. M. Tishler and C. Raffel, *J. Neurosurg.*, 1992, **76**, 502–506.
35 I. Notingher, J. Selvakumaran and L. L. Hench, *Biosens. Bioelectron.*, 2004, **20**, 780–789.
36 B. H. Long, S. T. Musial and M. G. Brattain, *Cancer Res.*, 1986, **46**, 3809–3816.
37 C. D. Bortner, M. I. Sifre and J. A. Cidlowski, in *Osmosensing and Osmosignaling*, Academic Press, San Diego, 2007, vol. 428, pp. 161.
38 S. Kumari, R. P. Rastogi, K. L. Singh, S. P. Singh and R. P. Sinha, *EXCLI J.*, 2008, **7**, 44–62.

